THE PENNSYLVANIA STATE UNIVERSITY
SCHREYER HONORS COLLEGE

DEPARTMENT OF CHEMICAL ENGINEERING

SYNTHESIS AND CHARACTERIZATION OF AMORPHOUS HYDROGENERATED CARBON NANOPARTICLES CREATED THROUGH PLASMA ENHANCED CHEMICAL VAPOR DEPOSITION TECHNIQUES

SRINATH YELAMARTY
Spring 2011

A thesis
submitted in partial fulfillment
of the requirements
for baccalaureate degrees
in Chemical Engineering and Economics
with honors in Chemical Engineering

Reviewed and approved* by the following:

Themis Matsoukas
Professor of Chemical Engineering
Thesis Supervisor

Darrell Velegol
Professor of Chemical Engineering
Honors Adviser

* Signatures are on file in the Schreyer Honors College.

ABSTRACT

The creation and behavior of carbon-based nanoparticles was investigated through plasma polymerization processes. Toluene and heptane precursors were introduced into a tubular reactor where Radio Frequency (RF) power was applied to the compounds, thus generating plasma and ionizing the components. Reassembling of the excited components can come in the form of films or particles. The goal of this work was to investigate the best experimental conditions for nanoparticle formation and to study these particles' colloidal properties.

In this work, when RF power was low (15W), both films and particles were generated. However, with greater time duration of test, came a greater ratio of particle formation. When RF power was high (40 & 60 W), only nanoparticles were observed—for all durations of testing. While heptane was used as a precursor for polymerization, it was observed that particles and films were both generated along the reactor wall. Furthermore, it was observed that heptane deposited higher amounts of product than toluene, allowing for ~0.1 g of product to be collected. Through sonication and separation techniques, the particles from heptane testing were suspended in solution and realized to be stable through Zeta Potential runs (-50).

Amorphous toluene particles were collected in the reactor filter while tests were conducted at low power (10W). These particles, initially 500 nm to 1 μm in diameter, experienced changes in morphology when exposed to a transmission electron microscope (TEM) beam. When exposed to the electron beam, the particles transformed from amorphous to a bubble-type hollow particle, greater than 1 μm in diameter. Furthermore, particles originating from heptane and toluene were tested for their hydrophobicity. It was observed that heptane based particles exhibited higher hydrophobic character than toluene based particles.

TABLE OF CONTENTS

ACKNOWLEDGEMENTS

I would like to give special thanks to Dr. Themis Matsoukas and Anaram Sharavan for their guidance through the research process. Anaram proved to be especially helpful in setting goals, working with me to complete the work, and helping me to understand the results. She also was responsible for capturing the TEM images seen throughout this thesis. Thanks also goes to the entire Dr. Matsoukas lab group; it is with their help and tutelage that this work and thesis was possible.

I would lastly like to acknowledge my family for their enthusiasm in my education while encouraging me to reach my maximum potential in all of my endeavors.

Chapter 1

Introduction

Overview of Plasma Polymerization

The field of plasma polymerization has become very prominent in both the research and industrial fields. The process involves exciting a gaseous monomer and in turn forming: electrons, radicals, excited molecules, and ions. The excitation of these monomers is based off a partial and/or complete ionization of the neutral molecules in the medium. There exist several ways to cause the ionization, they include: high ambient temperatures or an electric/magnetic field applied to the excitable molecules. In this work, hydrocarbon monomers (toluene and heptane) were mixed with an inert gas (Ar) and introduced into an electric field with the objective of producing nanoparticles. Since the hydrocarbon couldn't be excited to the plasma state alone, the Ar gas was excited first, allowing for the subsequent ionization of the monomer by using the Ar reaction as the needed activation energy.

Following the initial excitation of the hydrocarbon monomer, the components present in the plasma reassemble themselves into a polymer product, seen in Figure 1, and take on different properties and chemical behavior than the parent compound. This product has an amorphous structure and is formed through nucleation of the excited components. Furthermore, it should be known that the use of the word plasma is inherently misleading—plasma state has a characteristic glow (luminous gas phase); however, whether this phase created by an electrical discharge is in the plasma state is a very good question. In fact, it is hypothesized that major body of luminous gas phase is not in the plasma phase (1).

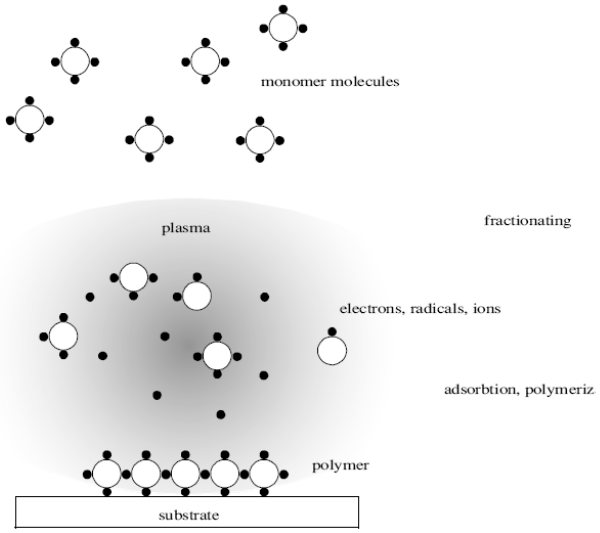

Figure 1 Formation of polymer product from monomer molecules (2)

Traditional methods use plasma polymerization to create a desired coating on a specific substrate—for example, thin film polymerization has been used to coat the inner-surface of plastic bottles by use of acetylene. Plasma enhanced chemical deposition (PECVD) is used to deposit metalized layers onto wafers in order to promote good conductivity in IC units. Furthermore, polymerized layers have applications such as scratch resistant coatings, corrosion protection and anti-bonding coatings. These types of depositions provide excellent coating adhesion on almost all substrates, high chemical and thermal stability, and have a high barrier effect.

Nanoparticle Generation

The nucleation of the excited components can come in a particle form or as a film/coating structure. As stated before, the goal of this work was to create carbon-based nanoparticles and correlate the particle characteristics to experimental conditions. These characteristics included: the ratio of the amount of particles to the amount of film generated, the size of the particles, the hollowness of the particles, among others. The carbon-based nanoparticle can come from a

variety of parent carbon based molecules. For this work, toluene and heptane were considered. Once a hydrocarbon is chosen, there are many other variable experimental conditions which can be altered to affect particle characteristics, they include: reactor pressure, flow rate of hydrocarbon introduced into the reaction, flow rate of inert gas, experimental duration and RF power given to the electrodes/plasma.

The creation of hollow nanoparticles has also been observed. These particles have come from hydrocarbon based depositions on silica particles which are then etched and removed, leaving a shell structure. Essentially, a template was set up and then removed leaving a shell structure. Hollow particles have also been noticed experimentally without use of a template. It is hypothesized that as a compound is ionized and starts to form a polymerized structure that the nucleation occurs closer to the boundary of the plasma of the spherical particle. Essentially, a void at the center increases in size leaving a hollow nanoparticle. It is seen in literature (3), that hollow particle formation is far from accidental and that many, though not all, organic molecules share to ability to produce such particles. The study, completed by Cao and Matsoukas, observed hollow particle formation for a variety of hydrocarbon precursors for experimental conditions of 15 W RF power, 400 mTorr pressure and 1:10 hydrocarbon-to-Ar partial pressure ratio.

Through previous studies completed, which used styrene as a precursor for polymerization, it is possible to see that nanoparticle size can be controlled through the operating conditions, namely, flow rate, partial pressure of styrene, and plasma pressure. Sizes generally increased with increasing mol fraction of styrene and decreased with increasing pressure (4). Through these findings, it is possible to hypothesize that varying the experimental conditions, in this work, should have an effect on the particle characteristics.

Hollow particles can have applications in drug delivery, plasmonics and catalysis (5). In drug delivery, a desired compound can be inserted into the center of the particle; this compound would then release through the digestive system and allow for a timed release of product. Nanoparticles also hold good applications in the heating and cooling liquids industry. Nanoparticles are characterized by a high surface area to volume ratio and also can be easily suspended in solution—creating a colloid. These characteristics allow nanoparticles to be good dissipaters of heat. Due to their low density and volume compared to micron sized particles, nanoparticles also cause less corrosion along fuel lines.

Particle Growth and Expansion

In order to verify the shape and size of the created particles and film, Transmission Electron Microscopy (TEM) proves to be a very important tool. TEM provides a resourceful tool to analyze the particles on the nanometer scale since differences in specimen density allow for changes in the contrast of images. While using TEM in this work, particle size and hollow characteristics have been verified. Furthermore, it was discovered that some particles, which used toluene as a parent monomer, were able to grown and form a bubble shape when exposed to the 120 keV electron beam. In literature (6) , it was observed that amorphous Fe and Fe Oxide nanoparticles evolved to core-shell structures under exposure to the beam of TEM. Using a prealigned 80 keV electron beam, it was possible to notice the growth of particles from the amorphous spheres to larger, hollow spheres. The change in geometry was directly linked to the irradiation. Furthermore, it was proven that the formation of these hollow spheres was in fact irreversible while growing from about 10.5 nm to 11.8 nm OD. This development of morphology occurred over the course of minutes and only to amorphous particles.

Due to the electron beam exposure, and not electron beam induced reduction, the results suggest that crystal defects or voids within the Fe oxide solid are necessary for the change in particle morphology. In essence, the change is credited to a phenomenon labeled quasi-melting. The process involves a fluid-like behavior of atoms or clusters of atoms to reach a thermodynamically favorable configuration (7). It is hypothesized that the energy barriers of reorganization are small and thus irradiation can provide the activation for the process to move forward (8). Data have shown that the increase in diameter occurs in an exponential fashion followed by a leveling off at long electron beam exposure times. It is hypothesized that the exponential growth follows a first-order process and is not dependent on temperature. The rate of change of particle structure was determined to be a function of particle size, current density of electron beam and the oxidation state of the metal atoms in the particle matrix (5).

Literature has also been published regarding the use of electron-beam lithography to create hollow structures (9). However, the original structure was a crystalline solid NaYF4:Yb,Er nanocrystal monolayer assembled into a close-packed hexagonal formation with a repeating unit of 21.6 nm. It was determined that when a TEM beam was targeted on a single particle in the monolayer, hollow structures of roughly the same outer diameter were formed. A small void was initially observed—this small void grew in size until a hollow center was noticed. Furthermore, under TEM testing, the sample was tilted to see the uniformity of the hollow shell. It was determined that the inner and outer diameter stayed constant throughout the hollow particle while the hexagonal assembly pattern was retained. The ability to grow allows these particles to be deemed “smart” particles. While it seems that a stable structure has been formed initially, the introduction of a radiation source provides the necessary energy to transform these particles into a new formation.

Stability and Characterization

TEM provided a valuable tool to characterize the results from toluene based polymerized structures. Furthermore, zeta potential was used to determine the stability of particles and films that were created while using heptane as the polymerization precursor. By suspending the generated product in a solution, the electrokinetic potential of the colloidal system can be determined. As zeta potential values approach zero, particles tend to aggregate. Essentially, as the absolute value of the zeta potential approaches zero, stability in the colloidal system decreases. Therefore, particles dispersed in solution with comparatively high or low zeta potentials are typically more stable.

The hydrophobicity of a sample can also provide insight to its characteristics. By placing a drop of water on the sample, the hydrophobic character of that sample can be determined based off the contact angle the water makes with the surface. As the hydrophobic character of a structure increases, so does the contact angle between the water and the film. This phenomenon can be explained by simple chemistry which dictates that repulsion forces between polar and non-polar substances would allow for less contact surface area between the water and the film, thus producing a greater spherical shape and a larger contact angle. It is regarded in literature (10) that any sample with contact angle greater than 60° can be labeled as a hydrophobic surface.

Chapter 2

Experimental Methods

The experimental setup was consistent for all tests completed. To begin, a Millipore filter was inserted in between the top and bottom parts of the reactor and the two pieces were then sealed closed using a clamp. The reactor was then evacuated of nearly all pressure; with the assistance of an Edward's roughing pump, the pressure was taken from atmospheric conditions to anywhere in the range of 20 mTorr to 200 mTorr. In order to produce plasma with the RF generator operating in the range of 10-100 W, low pressure is required. Two electrodes were situated around the reactor, each about 2 cm apart from each other. By using a process called capacitiviely coupled plasma (CCP), RF power was applied to one of the electrodes while grounding the other. The electric field then generated across the electrodes provided the necessary energy to ionize the components within the reactor. In this work, Ar gas was introduced along with the hydrocarbon since this noble gas could be excited given the RF power applied to the system as well provide the necessary activation energy to ionize the hydrocarbon.

Once a hydrocarbon was selected, it was placed in a water bath to properly maintain its temperature as it entered the reactor. Ideal conditions for nanoparticle creation were reached when the ratio of Ar gas to hydrocarbon entering the reactor was greater than a 10:1 ratio. By fixing the Argon flow to 12.8 sccm, it was possible to determine the optimal flow rate of the hydrocarbon based on the water bath temperature at which the hydrocarbon is immersed. Higher surrounding temperatures would push equilibrium towards greater vaporization and thus a greater amount of entering hydrocarbon into the reactor. For toluene, the ideal ratio was reached while Ar flow was kept at 12.8 sccm and the water bath was maintained at about 120-130°F.

For tests which included heptane as the hydrocarbon, a water bath temperature of 90-100°F was maintained. Once the pressure in the reactor had reached below 200 mTorr, it was determined that plasma polymerization could be feasible (any reactor pressure above 200 mTorr did not allow for plasma to be generated). At this time, a valve was opened allowing for the flow in of the Ar gas/hydrocarbon mixture through the top of the reactor. Given the semi-batch design, the inflow of gas would initially raise the pressure greater than 200 mTorr; however, within a short period of time (about a minute), the system would equilibrate and pressure would return to the acceptable range. A process flow of the experimental setup can be seen in Figure 2 below.

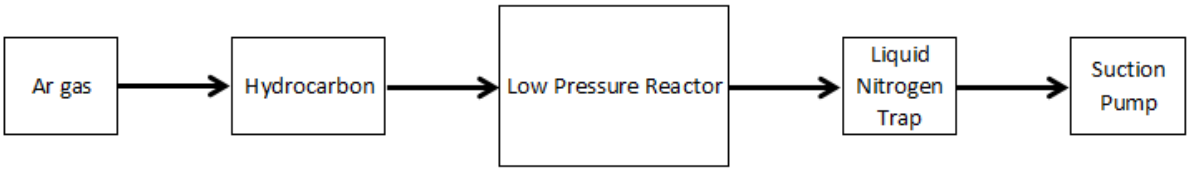

Figure 2 Block flow diagram of experimental setup

RF power was provided to the electrodes using a generator working with a matching box in order to ionize the entering components. The top electrode was powered while the bottom was one was grounded. Once the electrodes were attached and making good contact with the reactor, a control box was initiated first, followed by the RF power generator.

Following the ionization, excited ions, radicals and electrons would then nucleate together to form compounds that were chemically and physically different from the entering component. Essentially, from these ionized components, polymerization would occur to form film or particle structures. As seen in Figure 3 below, particles would be collected from around the electrodes and the filter in the reactor. The majority of the product was collected along the electrodes while a very minute amount was collected in the filter. Additionally, any unreacted

components would pass through the reactor and into the liquid nitrogen trap where waxy waste materials were collected. This trap provided a cryogenic atmosphere which allowed for condensation of unreacted components or polymerized structures which did not form particles or film. Essentially, the trap would keep impurities from entering the pump. If these components were to enter the pump, performance of the equipment would greatly decrease. In fact, poor pump performance would not allow for the environment of low pressure within the reactor, thus hurting plasma polymerization and experimental processes.

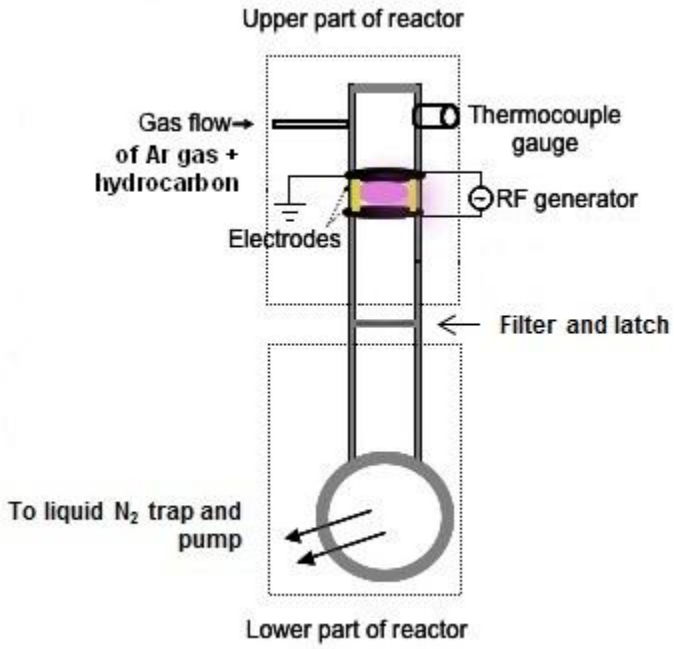

Figure 3 Experimental setup of reactor system

In order to collect created product, the system was removed from vacuum pumping and allowed to return to atmospheric pressure. The latch connecting the top and bottom portions was then removed, allowing access to both the filter and reactor wall. Since some of the created particles/film bonded to the reactor wall, they were removed by inserting a metal spatula into the top half of the reactor and scratching the surface. To ensure a clean reactor and repeatability of

tests, the reactor was physically cleaned with alcohol and chemically cleaned with oxygen plasma after every run. Also after each test, experimental logs were kept to keep good records of completed tests. An example of one of these logs can be seen in Table 1 below.

Down stream pressure before starting the experiment (read from pump barometer) (Torr)	2×10^{-3}
Down stream pressure before starting the experiment and after opening throttle valve (read from pump barometer) (Torr)	3×10^{-2}
Down stream pressure during the experiment (Torr)	1×10^{-1}
Reactor pressure before opening any valve (mTorr)	100
Reactor pressure after opening gas valve (mTorr)	150-200
Electrodes distance (cm)	2.5
Water temperature ($^{\circ}$F)	120-130
Initial liquid volume (mL)	25
Final liquid volume (mL)	6
RF power (Watts)	15 (20F, 5R)
Hydrocarbon	Toluene
Ar flow rate (sccm)	12.8
Experiment duration (min)	Overall: 22 Experimental: 20

Table 1 Example of Experimental Log

As stated before, once a hydrocarbon was chosen, there were many other experimental conditions which could have been adjusted, they included: reactor pressure, hydrocarbon flow rate, Ar flow rate, experimental duration and RF power given to the electrodes. Throughout testing, only the time duration and RF power were varied. There were also two times noted for a run: the overall time when hydrocarbon was introduced as well as the time of actual experiment (or the time which plasma was being generated). The overall time is the time from which the

reactor is opened to allow the hydrocarbon to enter until the experimental run is complete and the reactor is closed to any further entering components. The overall time was noted in order to determine the hydrocarbon flow rate (which was volume entered/time). The actual experimental duration is of most importance since it is the duration during which plasma polymerization occurs. Since plasma is not generated as soon as the hydrocarbon/inert gas mixture enters the reactor, the time before plasma and the polymerization process begins is referred to as the pre-experimental time.

Again, in this work, two different hydrocarbons were used for testing—toluene and heptane. For toluene, the following power and time durations were characterized, as seen in Table 2.

Experimental Duration (Minutes)	RF Power (Watts)
5	15
20	15
5	40
20	40
27	40
20	60

Table 2 Experimental conditions for tests run with toluene

For tests completed with heptane as a precursor, applied power varied from 45-50W. As a general note for this work, power applied to the system and experimental duration were maximized around 50 W and 30 minutes respectively.

Characterization of Particles

For applied RF power lower than 40 W, particles formed within a film structure. In order to test the characteristics of these trapped particles, sonication via a cleaning sonicator was completed for up to 30 minutes to separate the two components. The sonicator provided high intensity sound energy to agitate and disrupt the sample causing large aggregations to break apart easily while in solution. This sonic energy should theoretically provide the necessary energy to break apart the particles from the films. A sample collected from the reactor wall was placed in a 20 mL vial along with a solvent (water and ethylene glycol). Due to the low densities of the solute, a suspension can be created when the particle/film mixture is placed in solution. By placing the solute/solvent mixture in a water bath system with ultrasound generating elements below, high intensity waves were transmitted into the compound. By passing a laser beam through the sample after sonication, it was possible to qualitatively test the dispersion of the particle/film mixture and thus check if large film aggregations were still present in solution.

Sonicated samples could undergo zeta potential testing to determine stability of the dispersed particles. TEM testing allows for the ability to view the collected product on a microscopic scale. Using a 120 keV aligned electron beam, images were taken of the microscopic samples using scale ranges of 10 nm up to a micron. TEM images showed the distribution of particles to film within the sample, but also provided the diameters of the particles generated through plasma polymerization. It was also determined whether the particles were hollow or not by viewing the darkness of the interior. A hollow particle had less density in its center, allowing for greater passage of electrons through to the imaging device. This difference in density lead to a lighter shade at the center of the image while a darker shade around the edges.

As stated before, products of the reaction could be collected along the reactor wall or in the filter. The product along the filter was collected using two methods: by either brushing a TEM grid across the filter or by washing the filter with water and subsequently placing a TEM grid in the nanoparticle/water mixture. Nanoparticles collected along the filter, which were based off toluene and polymerized at low power (<15W), saw particularly interesting and surprising results. It was determined that these nanoparticles expanded in size while morphing from an amorphous solid to a hollow bubble structure when exposed to the 80 keV electron beam of TEM. Videos of the expansion were taken in order to characterize the growth over time of the particles.

Hydrophobicity testing was also completed on the polymerized structure. However, measuring the hydrophobic characteristics of plasma polymerized nanoparticles can be difficult to complete—especially when less than 0.1 g of product is being created through the reaction. An appropriate method to test the hydrophobicity was the devised by placing a silicon wafer into the reactor near the electrodes (the region where the most particles and film are formed). As the reaction proceeded, the wafer acquired a thin coating, similar to PECVD processes. This wafer was then tested using a contact angle measurement device. A drop of water, approximately 1 μL, was placed on the wafer and a CCD camera took a picture of the water droplet on the surface. As stated above, by measuring the angle between the water and the contact surface, the hydrophobic character of the polymerized was determined.

After noticing that particles made from toluene collected along the filter could be excited using a high energy electron beam, various other forms of electromagnetic radiation were administered to the particles to test their effect. The product was collected, placed in a testing vial, and dispersed in water as before. The solutions were then exposed to a variety of various

sources of electromagnetic radiation in attempt to excite the particles. These forms of radiation included: a 60 mW HeNe laser, a 100 mW Ar laser, a 200 mW Ar Laser, and UV Light. Also, a voltage was applied across the sample using a DC source. As seen in Figure 4 below, the voltage was applied across the sample then transferred across a bridge and a salt solution before completing the circuit back to the source.

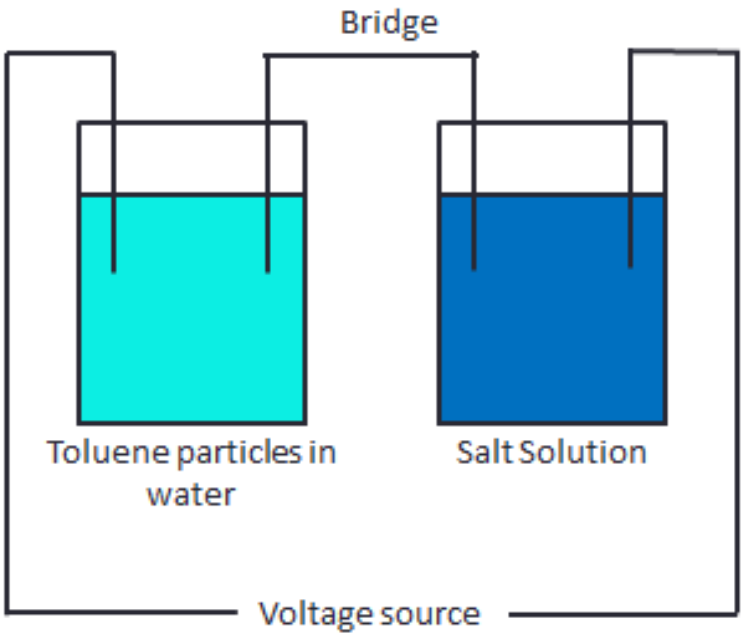

Figure 4 Voltage testing setup

Chapter 3

Results and Discussion

Toluene Testing

A large objective of this work focused on correlating experimental conditions to the characteristics of the product that was created and deposited on the reactor wall. Product characteristics included: the ratio of the amount of particles to the amount of film, the size of the particles, the hollowness of the particles, among others. These characteristics were based on the changing experimental conditions of both testing duration and RF power applied to the system during plasma polymerization. When toluene was used as the hydrocarbon precursor, it was determined that the ratio of particle to film generation was maximized at high applied power, around 40-60 W. It was also determined that at low powers, around 15 W, the ratio of particles to film increased with longer experimental durations. In this work, the maximum experimental duration was around 20 minutes, while most toluene tests provided less than 1 milligram of product.

Experimental testing started at a low power of 15 W and at a time duration of 5 minutes. Under these conditions, a mixture of both particles and film were observed, as seen in Figure 5 below. Diameters of particles were approximately 30 nm and were often embedded in a film structure or an aggregation. Clusters of particles were also noticed, as seen in Figure 5b. Furthermore, particles that were created had both hollow and non-hollow structures. Under these conditions, 14 mL of toluene were introduced into the reactor over the course of 17 minutes (overall experimental run) resulting in a 0.8235 sccm flowrate of toluene. Since Ar gas was

maintained at a 12.8 sccm flow rate, the ratio of argon gas to hydrocarbon entering the reactor was determined to be 15.54:1, greater than the 10:1 ratio required to polymerize particles.

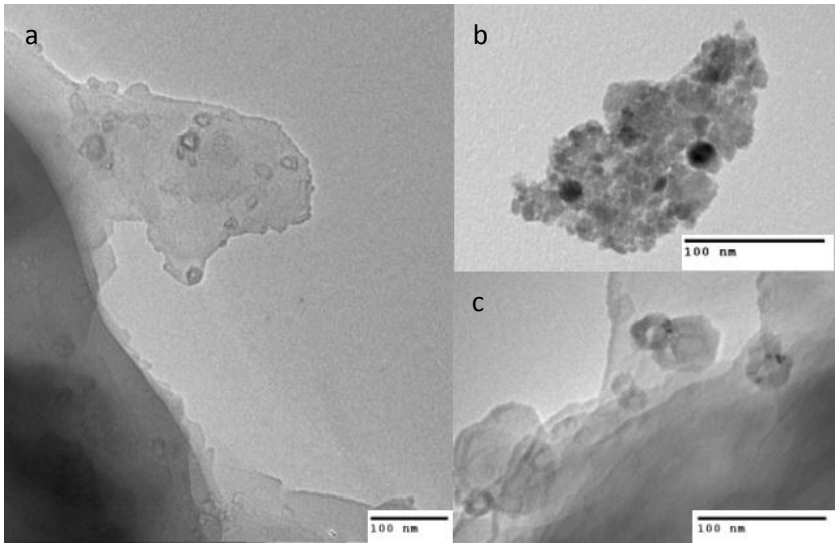

Figure 5 (a,b,c) TEM images taken of product from reactor wall with 15 W plasma with 5 minute experimental duration

While continuing toluene testing at 15W, the experimental duration was increased to 20 minutes. Under these conditions, the size of the particle diameter was approximately 20 nm in size. It is theorized that the larger particle size was due to the longer length of test; under these conditions, there exists more time for nucleation, particle deposition, and growth of structures. As was seen in the 5 minute run, clusters of particles with diameters of about 20 nm were also observed; Figure 6 below shows the hollow particles embedded in a film. Over the course of this run, 19 mL entered into the reactor over 22 minutes resulting in a 0.864 sccm of toluene. Ar gas was once again maintained at 12.8 sccm—corresponding to an Argon gas to toluene ratio of 14.82 entering the reactor.

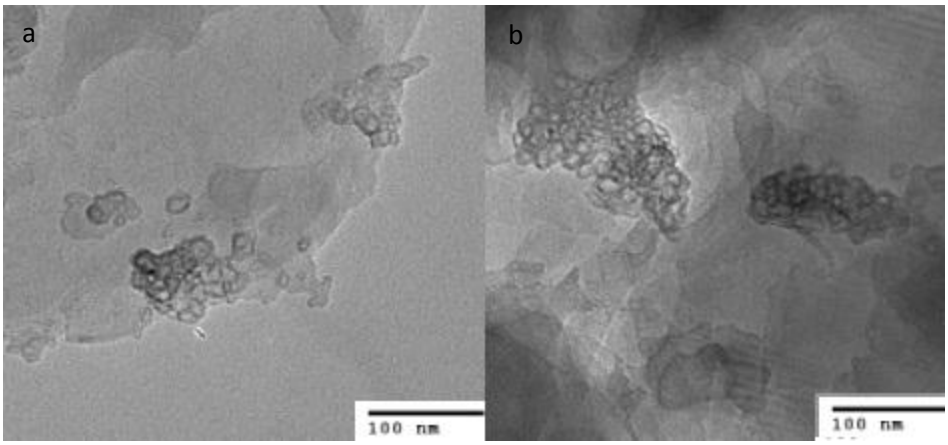

Figure 6 (a,b) TEM images taken of product from reactor wall with 15 W plasma and 20 minute experimental duration

Testing power was increased to 40 W while the plasma polymerization was completed again for five minutes. The results of this trial can be seen in Figure 7 below. At this power and temperature, it was determined that mostly particles were formed along the reactor wall. As seen in the figure below, diameters of the particles ranged from 5-20 nm. Furthermore, it was noticed that hollow particles were once again generated as well as non-hollow particles.

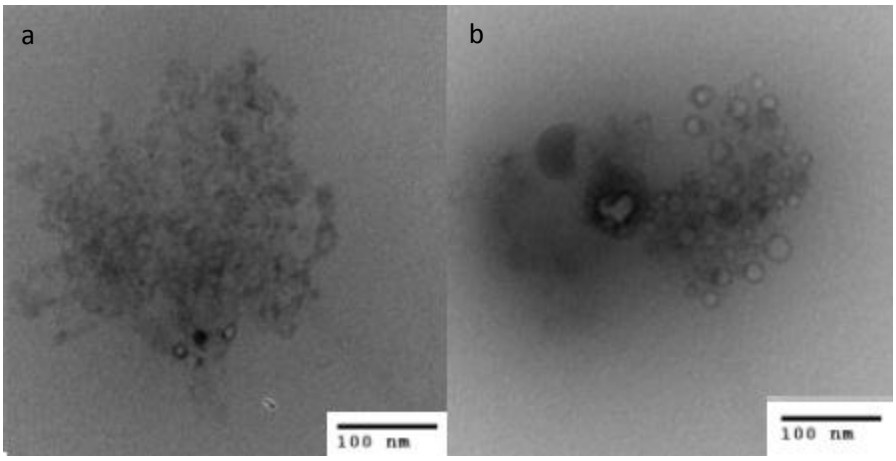

Figure 7 (a,b) TEM images taken of product from reactor wall with 40 W plasma and 5 minute experimental duration

While continuing to apply 40 W to the system, the experimental duration was increased to 20 minutes. As seen in Figure 8 below, particles size diameters of 5-10 nm were observed (as

seen encircled). There were also regions which exhibited properties of oiliness or waxiness (seen in squares below) when a TEM image was taken of the sample. These regions could have been the result of the non-polar toluene monomers which morphed into larger structures but not into a particulate or film structure; these regions are not thought to be a type of contamination. Furthermore, only particles, and not films, were observed at these experimental conditions. However, very little product was generated through testing—much less than other experimental runs.

At the start of this 40W and 20 minute run, the pressure inside the reactor was 200 mTorr. However, as the 20 minutes of experimental run passed, the pressure was unable to be maintained at 200 mTorr and increased up to 600 mTorr by the end of the run. This increase in pressure could be attributed to poor pump performance during this specific test. As stated earlier, plasma polymerization for this experimental setup is dependent on the reactor operating at a pressure below 200 mTorr. Therefore, the increase in pressure could attribute to the results observed under TEM for this product sample. The lack of proper low pressure could have attributed to the waxy regions that were observed because of improper or incomplete polymerization of the parent structure. Also based on the same reasoning, the high pressure could explain why very small amounts of product were generated.

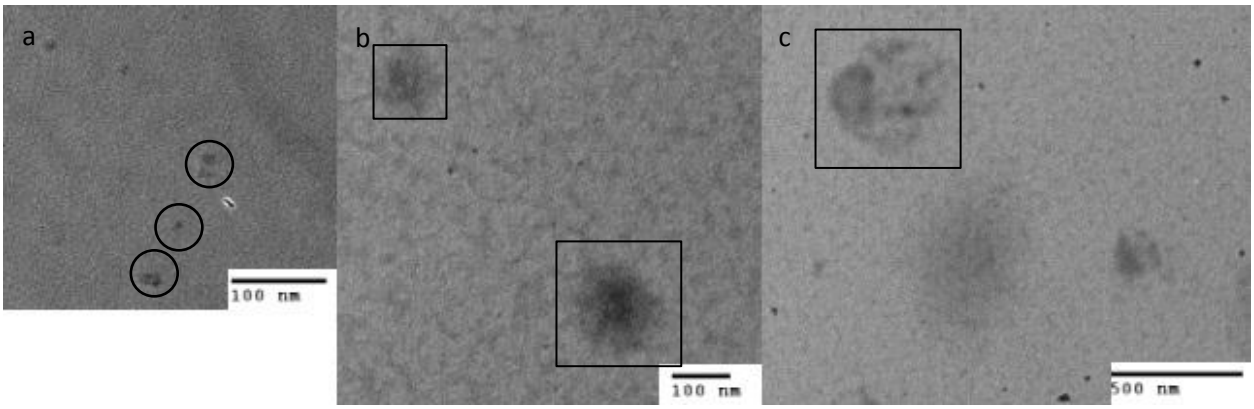

Figure 8 (a,b,c) TEM images taken of product from reactor wall with 40 W plasma and 20 minute experimental duration

Experimental testing for toluene was also completed at 40 W with an experimental duration of 27 minutes. The generated particles can be seen in Figure 9 below. Over the course of this run, 19 mL were entered into the reactor over 33 minutes resulting in a 0.576 sccm of toluene. Ar gas was once again maintained at 12.8 sccm—corresponding to a toluene to Ar flow rate of 1:22.13.

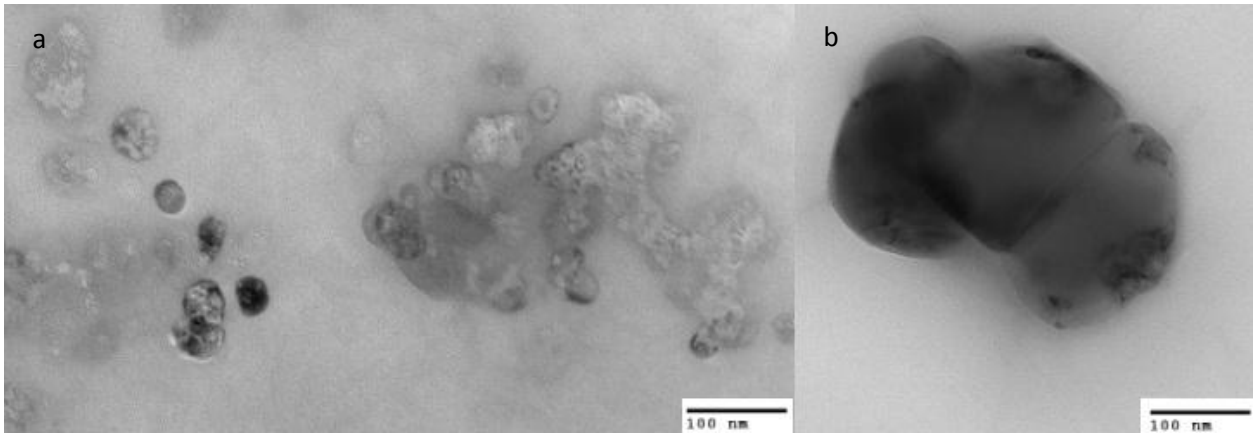

Figure 9 (a, b) TEM images taken of product from reactor wall with 40 W plasma and 27 minute experimental duration

The applied power to the reactor was increased to 60 W and the experimental duration was kept at 20 minutes. A TEM image of the collected product can be seen in Figure 11 below. Once again, at high powers, nearly all particles were collected in the product. As seen in Figure

10, the diameter of the particles ranged from 5-15 nm in size. Furthermore, it seems that most of the product was composed of hollow particles rather than filled.

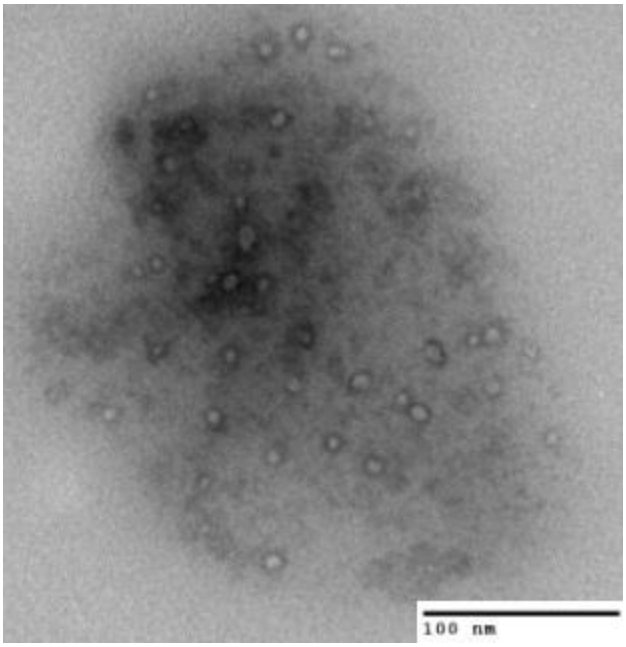

Figure 10 TEM image taken of product from reactor wall with 60 W plasma and 20 minute experimental duration

In conclusion, for tests which used toluene as a precursor, it is possible to conclude that higher powers (40W and 60W) promote the formation of particles instead of films. Lower power, less than 30 W, promote the growth of both particles and film. At these low testing powers, longer experimental durations promoted a higher ratio of particles to film. Table 3 below shows the experimental characteristics which promote the generation of either particles or film. For most high power tests, the particle size ranged from 5-20 nm, while sometimes exhibiting hollow characteristics. At this time, it is unsure why hollow particles are formed since they exist for all pressures and time durations of tests. It is possible that conducting plasma polymerization with toluene produces a mix of hollow and non-hollow particles. Furthermore, it seems that the particles are often poly-dispersed with various diameters generated for each test

condition. These particles, usually not perfectly circular, share surfaces with a neighboring particles or are embedded in a film.

	5 min	20 min	27 min
15 W	Film and Particles	Film and Particles	
40 W	Particles	Particles	Particles
60 W		Particles	

Table 3 Summary of results of toluene based plasma for varying experimental conditions

Heptane Testing

As stated before, heptane was also a precursor hydrocarbon used in the plasma polymerization process. Two separate tests were run with heptane, both applying 50 W of RF power for 30 minutes of experimental time. Product was collected from the reactor wall. A strong contrast between the toluene and heptane tests was the amount of product collected. While toluene based plasma generated less than 1 milligram of polymerized product, heptane plasma created about 0.1 g of product. Figure 11 at first view looks like a film structure.

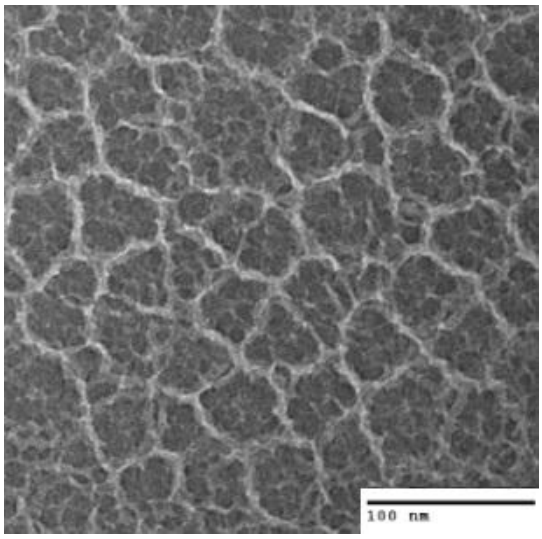

Figure 11 TEM image taken of product from reactor wall with 50 W plasma and 30 minute experimental duration

However, with greater zoom it is possible to see that the product taken from the reactor wall is made up of many polydisperse particles agglomerated together in a film (as seen in Figure

12). Since the product of heptane tests was initially dissolved in a solvent water, the aggregation of particles could be described by solvent which evaporated leaving this structure behind. The natural formation of the particle/film mixture during polymerization provides another explanation for the TEM image seen below.

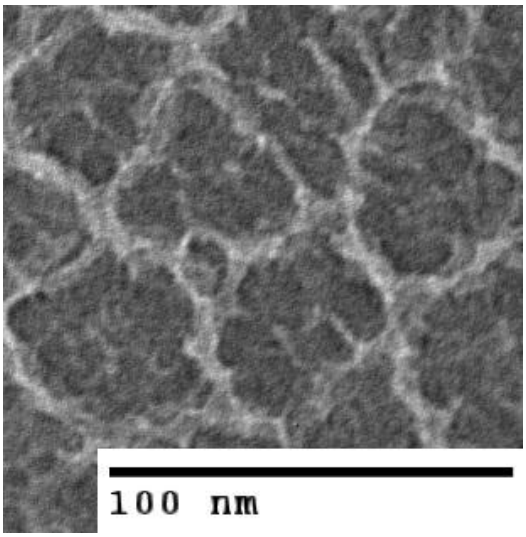

Figure 12 A closer look at heptane based plasma polymerized particles

After collected the polymerized product from the reactor wall, it was dispersed in solvents of either ethanol or ethylene glycol. In order to separate the particles from the aggregation and film, sonication methods were employed. A vial of the particle/solvent mixture was placed in a cleaning sonicator for a period of 30 minutes. After this process was complete, zeta potential testing was completed to determine stability of solution. In completing these tests, the solution was taken from the top of the vial as to not include all of the heavier films which were removed from the particles in the sonication process. For heptane particles dispersed in ethylene glycol, the zeta potential of the solution was determined to be -51.35 and -51.39. From these values, it can be concluded that this solution was of good stability. Alternatively, when ethanol was used as the solvent, the zeta potential of the solution was determined to be -29.29, showing small amounts of stability. The initial pH of the heptane particles was 4.78; however, as the pH was

lowered to 2.16 with an HCl solution, zeta potential was -5.89, showing coagulation of particles. Therefore, heptane particles dispersed in ethylene glycol provided the greatest stability, while particles dispersed in ethanol were less stable, particularly at low pH.

Hydrophobicity Testing

In order to gain a greater understanding for the particles that were created, hydrophobicity testing was completed. However, as stated before, testing the hydrophobic character of nanometer sized particles poses some difficulty. Therefore, a silicon wafer was introduced into the reactor, near the electrodes, during the plasma polymerization process. By allowing this wafer to obtain a thin coating, the hydrophobicity of the particles could be correlated to the contact angle between the coated wafer and an applied droplet of water. The silicon wafer by itself proved to be hydrophobic as the contact angle was determined to be 108.56° as seen in Figure 13 below.

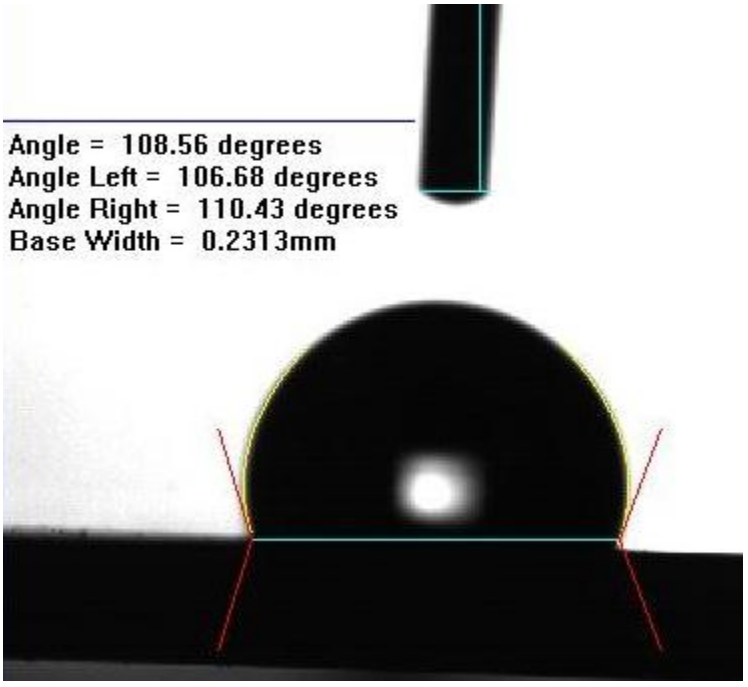

Figure 13 Contact angle measurement between water and silicon wafer

The silicon wafer was then introduced into the reactor during toluene based plasma runs; this plasma was run at 10 W for an experimental duration of 5 minutes. Three different contact angles were observed between the wafer and the water droplet (80.11°, 75.14°, and 83.49°) with an average contact angle of 79.58°. A sample run for toluene can be seen in Figure 14 below. Since the average contact angle between the wafer and the water droplet was greater than 60°, the toluene based polymerized structure can be said to be hydrophobic as well.

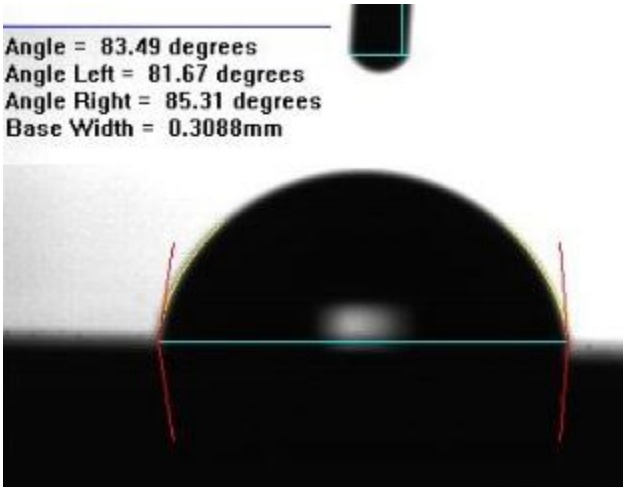

Figure 14 Contact angle between toluene based deposition and wafer

The silicon wafer was also introduced into heptane based plasma (which was run at 50 W for an experimental duration of 30 minutes). Four different contact angles were recorded for this test, they were: 100.42°, 89.46°, 97.26°, and 97.53°. Therefore, the average contact angle between the heptane based film and the water droplet was determined to be 96.17°. A sample run for heptane can be seen in Figure 15. Once again, the structure was determined to be hydrophobic.

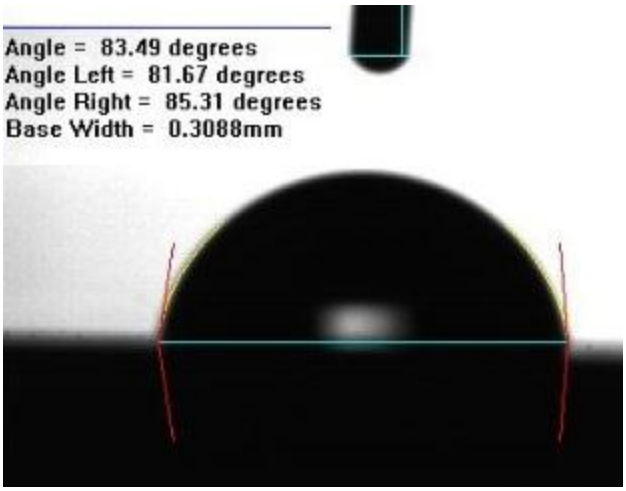

Figure 15 Contact angle between heptane based deposition and wafer

The polymerized structures of both toluene and heptane proved to be hydrophobic. Through the data presented above, it is possible to determine that the heptane based structure had a higher hydrophobic character than the toluene based structure.

Bubble Particle Generation

As stated earlier, particles generated through toluene based plasma polymerization had the ability to change morphology when irradiated with a TEM beam. The change in morphology was characterized by growth in overall particle size and by growth from a filled particle to a hollow particle. Figure 16 below shows the transformation of the particles into bubble type structures. Furthermore, it was determined that the only particles capable of excitation/growth under TEM exposure must have fit the following experimental specifications: created from toluene precursor, excited under low power (<10W), and collected along the filter. These bubble particle results are presented with great excitement since such "smart" particles are a very new discovery in the field of nanoparticles. In fact, this work is the first to report particles capable of such growth while originating from a carbon based molecule.

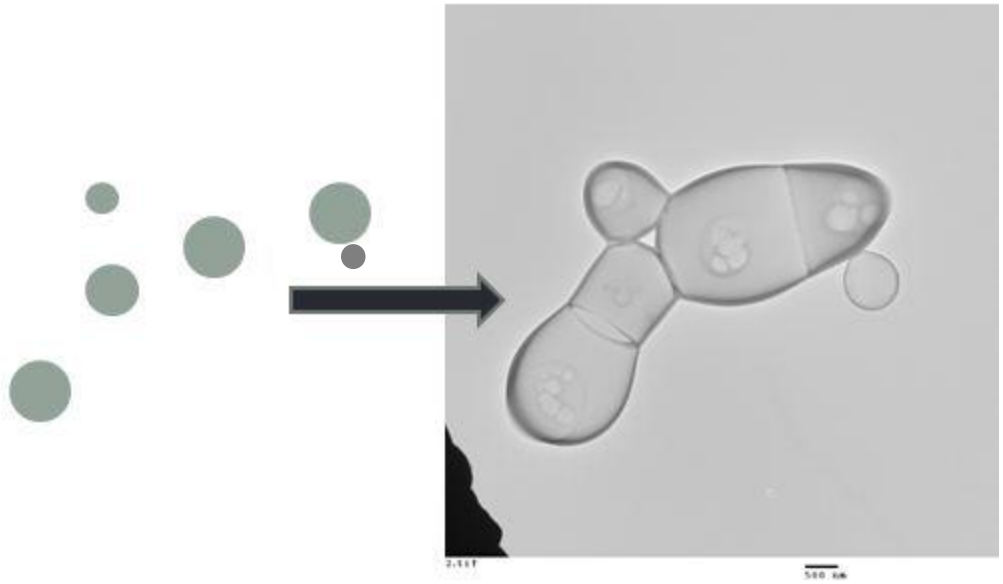

Figure 16 Growth of particles into bubble structure

As seen in Figure 16 above, the grey circles (on the left) represent the particles before growth. The size of the original particle can be determined by the smaller circular shape located at the center of the bubble particle. This interior circular region represents both the original particle size as well as the region which is still in contact with the TEM grid post expansion. Furthermore, since the growth of the particles to their hollow structures did not occur instantaneously under TEM exposure, a time dependent figure of the expansion can be generated. Figure 17 below shows the development of a particle over 12.5 seconds as it is exposed to the electron beam.

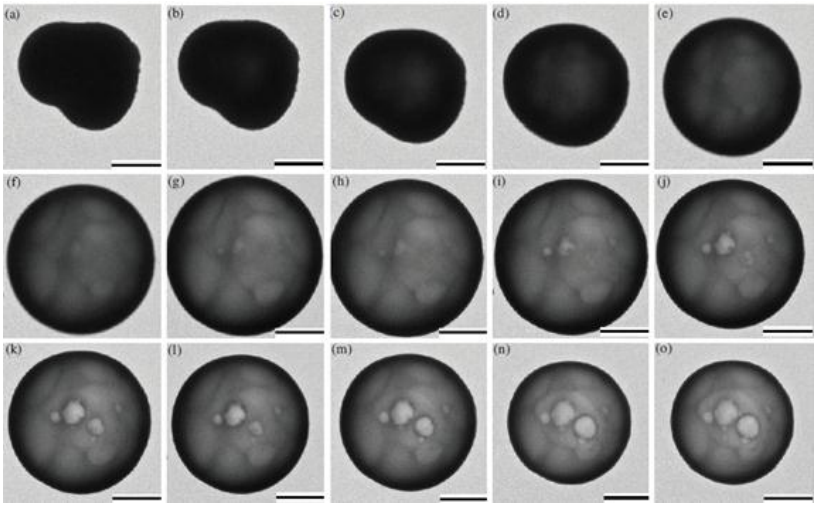

Figure 17 Growth of particle while exposed to 120 keV TEM beam for durations of (a) 0.6, (b) 0.8, (c), 0.9, (d), 1.26, (e) 1.4, (f) 1.5, (g) 1.6, (h) 2, (i) 2.4, (j) 2.9, (k) 3.3, (l) 4.43, (m)8.7, (n)11.2, (o) 12.5 s

The attachment of the inner circle in the bubble particle to the TEM grid can be proven through Figure 18. Through rotation of the sample holder, alternate views other than top-down can be seen.

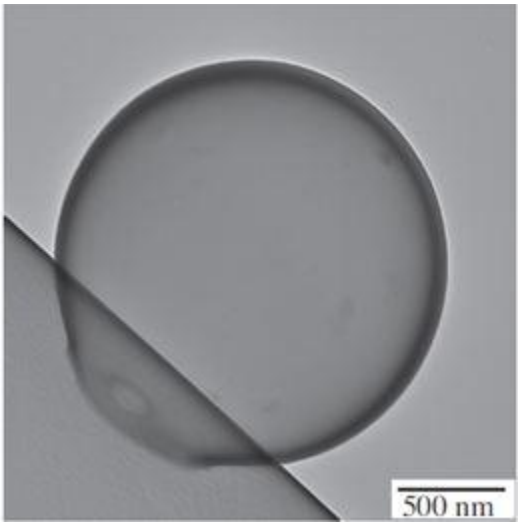

Figure 18 TEM image of hollow particle attached to the carbon film on the TEM sample holder

The electron beam provides the activation energy to transform the collected particle into a hollow and larger structure. It is hypothesized that the 120 keV beam excited the contents in

the interior of the particle or a gas trapped within. The goal of this work was to primarily document the occurrence of these hollow/bubble structures since it is still not fully known why such excitation and expansion occurs for these particles. Starting at about 500 nm in diameter, the amorphous structures expanded to more than 4 μm in size. A remarkable characteristic of the hollow particle is the stability after expansion. Once the particle is removed from electron beam exposure, it stays in the expanded structure and does not fall back to its original "state". It is also interesting to note that even at these experimental conditions, the only particles capable of this growth were collected from the filter and not the reactor wall.

Alternate methods of stabilization for toluene based nanoparticles

After discovering the effect of the TEM beam on toluene based nanoparticles, various other forms of energy were tested to see if they would have a similar result. Essentially, the objective was to find alternative methods which provided the necessary excitation to form a new stable formation. This formation could have been similar to the one observed after TEM or a completely different one. Various forms of electromagnetic radiation were believed to bring about excitation; therefore the particles were exposed to the following types of EM radiation: a 60 mW HeNe laser, a 100 mW Ar Laser, a 200 mW Ar laser, and UV light. In addition to these forms of energy, 5V of electricity was passed through particles dispersed in a solvent in attempt to create excitation. A difficulty in completing this testing was distinguishing which expansions occurred under TEM exposure and which occurred due to the alternate energy source provided. However, due to the directness of the 120 keV electron beam, if a hollow particle didn't expand while being observed through the viewfinder, it can be said that the structure was based on an alternate form of energy (listed above).

To begin, the particles were first viewed under optical microscope. Figure 19 below shows particles before TEM radiation as well as after; the size growth and hollowness of the particles can be easily distinguished from one image to the other.

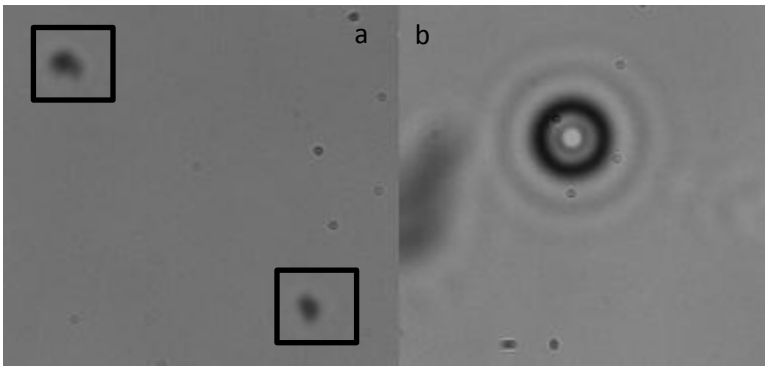

Figure 19 Nanoparticles under light microscope a) before TEM expsoure b) after TEM exposure

As the particles were exposed to the 60 mW HeNe laser, they did not the experience excitation that was observed when placed under the electron beam. After exposure to the TEM beam (following the HeNe laser), the particles formed hollow structures as they did before, as if the laser had no effect on them. Figure 20 below shows a bubble particle first exposed to the HeNe laser and consequently placed under TEM beam, the latter of which caused the expansion.

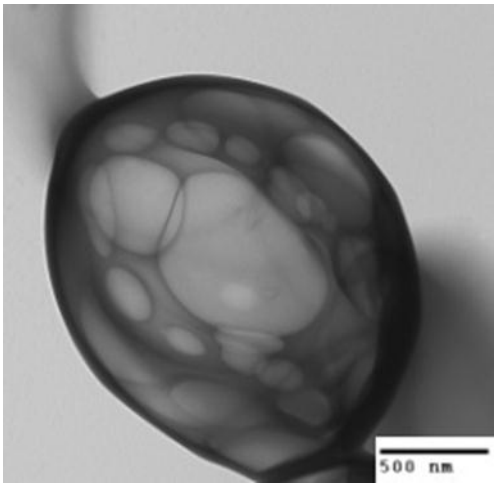

Figure 20 TEM image of stabilized nanoparticle after exposure to 60 mW HeNe laser and electron beam

Exposure of the toluene based nanoparticles to a 100 mW Ar laser caused formational changes in some, but not all of the particles. Even after exposure to the 100 mW laser light, some nanoparticles in the sample were able to form bubble structures when exposed to the TEM beam. Figure 21 shows a particle or group of particles which have stabilized into the formation seen below. Even with TEM exposure, this structure did not change its shape or characteristics.

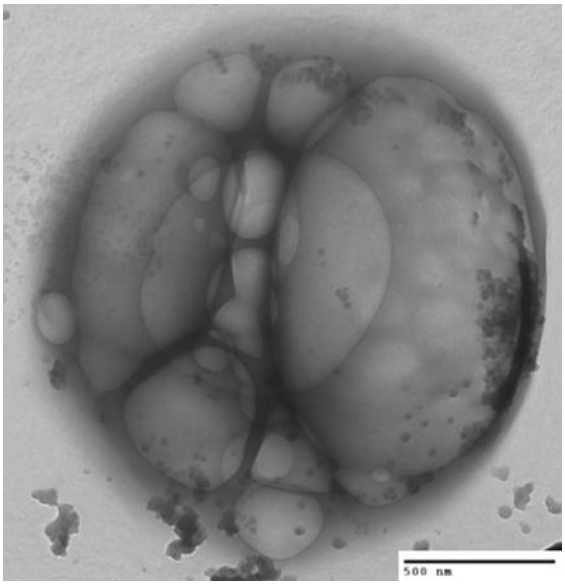

Figure 21 TEM image of nanoparticle after exposure to 100 mW Ar laser

By exposing the sample to a 200 mW Ar laser, a greater amount of particles were stabilized in comparison to tests run with the 100 mW Ar laser. While bubble structures were formed, they formed a bit differently than the ones under TEM. Viewing Figure 22a, it is possible to see a cluster of toluene based particles stabilized by Ar laser exposure. Figure 22b shows a hollow bubble structure formed which appears to be a group of particles formed together. In these structures, there were not any individualized hollow particles observed as were generated under the TEM beam.

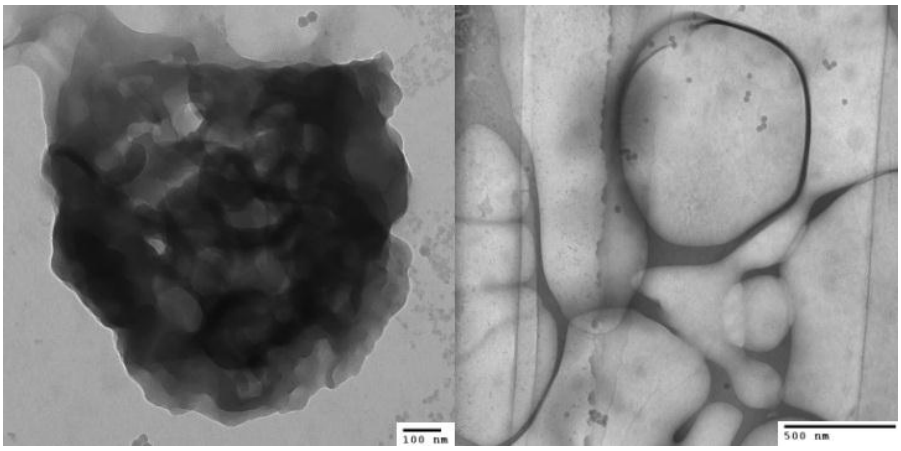

Figure 22 TEM image of a) cluster of particles stabilized under 200 mW Ar laser exposure b) an agglomeration of bubble structures formed by 200 mW Ar laser

Ultra Violet light did not excite the particles to a hollow structure like the electron beam. However, the UV light did provide the necessary energy to transform the structure of the amorphous compound. By viewing Figure 23 below, it is possible to see that the particle has breaks along its exterior. Also, when this particle was irradiated with the electron beam, it did not change shape nor was affected by the electron beam.

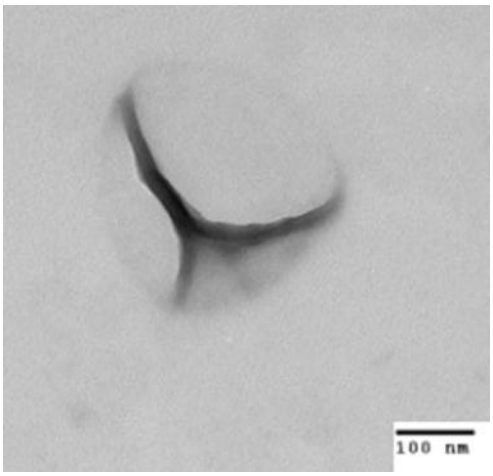

Figure 23 TEM image of nanoparticle after UV exposure

The final type of energy provided was an applied voltage across a mixture of water and nanoparticles. Using the experimental setup seen in Figure 6, 5 V was applied to the sample for a period of 25 minutes. After this testing, characterization using TEM was completed (generating Figure 24 seen below). As voltage was passed across the sample, the particles gained a level of stability and formed the structures seen below. As the electron beam was passed through the sample in TEM testing, it was noted that the structures remained in their formation and did not change their structure. From this observation, it can be said that an applied voltage has an effect on the overall stability of the product.

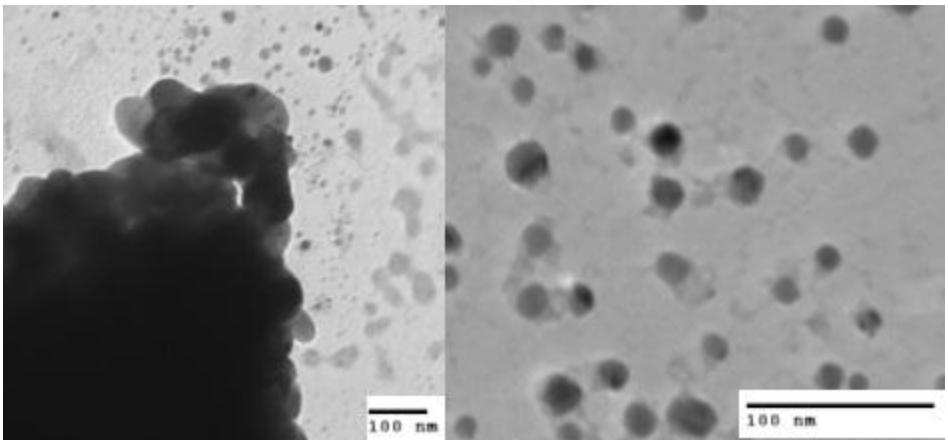

Figure 24 TEM image of particles after applying 5 V to the sample

Overall, this specific set of tests provided good insight into which types of energies allow for the stabilization of the toluene based nanoparticles. As discussed above, the 60 mW HeNe laser was not observed to have an effect on the particle structure. However, the 100 mW Ar laer, 200 mW Ar laser, UV light and applied voltage all provided some stabilization for the structure. These alternate forms of excitation represent a good progress in the realm of "smart particles". Since laser light and voltage are much more common and accessible than the electron beam of a TEM device, finding a form of energy which induces similar effects can be a very important advancement in this field.

Chapter 4

Conclusions and Future Work

Conclusions

This thesis studies the creation and behavior of plasma polymerized, carbon based nanoparticles created in a low pressure system. As stated before, the applications of both plasma polymerization and nanoparticles have attracted attention in their respective fields. In this work, toluene and heptane were used as a precursor to a polymerized product which was either nanoparticles or films. A main goal of this thesis was to determine which experimental conditions promoted the formation of nanoparticles. This work used two main experimental variables: RF power applied and experimental duration. Using toluene as a precursor, high power applied to the reactor (>40W) allowed for the creation of particles. Also, at low power (<15W), it was determined that a greater amount of nanoparticles were formed at longer experimental durations. For all tests using toluene, about 1 milligram of product was generated. When heptane was used as the precursor for plasma polymerization, it was found that a greater amount of product was created—about 0.1g. Also, when the heptane based particles were dispersed in solution, they were determined to be stable through zeta potential testing (-50).

Hydrophobicity testing provided another way to characterize the particles that were created. While the actual particles weren't tested, a silicon wafer coated under the same experimental conditions as the generated particles was tested. A water droplet was placed on the wafer to determine the contact angle between the droplet and the wafer. While both toluene and heptane based coatings were determined to be hydrophobic, the wafer coated with a toluene based structure had an average contact angle of 79.58° while the heptane based coating had an

average contact angle of 96.17°. From this result, it was determined that heptane based polymerized structure had a greater hydrophobic character than the toluene based structure.

An interesting result documented in this thesis was the creation of bubble particles. When the particles generated from toluene under low power were placed under TEM, they grew in size and became hollow. It is hypothesized that the 120 keV electron beam excited the contents in the interior of the particles causing the hollowing and growth in size. The electron beam provided the activation energy for the particles to reach a more stable state. Even after the particles were removed from TEM, the structure remained as it was post excitation and did not fall back to the original formation. In an effort to gain more insight into these results, alternate types of energies were provided to see if they could provide similar growth and excitation. Using a 60 mW HeNe laser, a 100 mW Ar laser, a 200 mW Ar laser, UV light as well as a voltage applied the sample, testing was completed. It was determined that alternate sources of energy could provide the activation energy necessary to stabilize the particles. With the exception of the HeNe laser, once the particles were placed under the exposure of these alternate sources, they formed new structures which were then unaffected by the TEM electron beam.

Future Work

Future work would entail gaining more insight into the sizing of the particles. Dynamic Light Scattering (DLS) was attempted many times in order to obtain a more accurate value of the particle diameter. However, a concrete number was never established. The particles could have been too polydispersed or still embedded in a film structure. This study sonicated particles dispersed in solution for 30 minutes and placed the sample in a centrifuge to remove the larger film components, but a value through DLS was never achieved. With more sonication and centrifuging, a value for particle diameter through DLS could be achieved. Also, heptane tests

could be expanded to determine optimal power and experimental duration for creating nanoparticles. Regarding the bubble particle formation, future work could start to determine why the hollow particles are forming. Furthermore, various other forms of energy and EM radiation could be tested on the toluene based particles to see the effects.

Bibliography

1. Yasuda, H. *Luminous Chemical Vapor Deposition and Interface Engineering*. New York: Marcel Dekker, 2005.

2. Plasma Polymerized Coatings." Midwest Tungsten Service. <http://www.tungsten.com/tipspoly.pdf>.

3. Cao, J.; Matsoukas, T. *Journal of Nanoparticle Research 6*: 447–455, 2004

4. Dongsheng, L.; Raymond, V.; Shahravan, A.; Matsoukas.; *Journal of Nanoparticle Research 13:* 985-996, 2010

5. *Langmuir*, 2008, *24* (24), pp 14195–14202

6. *J. Am. Chem. Soc.*, 2006, *128* (39), pp 12632–12633

7. Marks, L. D. *Rep. Prog. Phys.* 1994, 57, 603-649

8. Sun, S.; Zeng, H.; Robinson, D. B.; Raoux, S.; Rice, P. M.; Wang, S. X.; Li, G. J. Am. Chem. Soc. 2004, 126, 273-279

9. Feng, W.; Sun, L.; Zhang, Y.; Yan, C.; *Small*, 5: 2057-2060, 2009

10. *Langmuir*, 2009, *25* (24), pp 14105–14115

ACADEMIC VITA of Srinath Yelamarty

Srinath Yelamarty
1057 Treeline Drive
Allentown, PA 18103
SriYelamarty@psu.edu

Education

The Pennsylvania State University
Schreyer Honors College, University Park, PA

College of Engineering

Major: Chemical Engineering
Expected Degree: B.S. in Chemical Engineering with General Option

Liberal Arts College

Major: Economics
Expected Degree: B.S. in Economics

Research Experience

Dusty Plasma Laboratory, Undergraduate Research Assistant under Dr. Themis Matsoukas
Fall 2009 – Present

III-V Photonics Laboratory, Lehigh University, Research Assistant under Dr. Boon Ooi
May 2008 – August 2008

Work Experience

Procter & Gamble, Summer Engineer, Mehoopany, PA,
Summer 2009, Summer 2010

LASERVY Corporation, Engineering Trainee, Allentown, PA
Jan 2006—August 2008

WDIY Radio, Youth Media Correspondent, Bethlehem, PA
Sept 2003—May 2007

Awards

- Dean's List

Activities

- Atlas THON Merchandising captain for THON 2009
- Donor Relations Captain for THON 2010
- Supply Logistics Captain for THON 2011